- Specimens for use in cantilever reverse-bending tests with tapered widths (Fig. 14c)

Flat specimens generally are clamped in flat wedge-type grips or may be held with a stiff bolted clamp/joint friction grip for reversed axial loading. Pin loading can be used when only tensile loads are encountered. When pin loading is utilized, the holes drilled in the grip end must be designed to avoid shear or bearing failures at the holes, tensile failure between the holes at maximum load, and fatigue cracking at the holes in the grip end. In axial fatigue testing of flat sheet specimens, the test length and cross section must be designed to prevent premature buckling of the specimen.

Alignment Considerations

The keys to achieving accurate fatigue data include ensuring that applied loading is aligned with the specimen axis. This is particularly important in axially loaded specimens. Poor and nonreproducible alignment produces bending strains that reduce the fatigue life and increase the scatter in the data. In fact, it has been calculated that the largest contributing factor to scatter in LCF data is due to bending (Ref 21). Bending strains arise when there is a misalignment somewhere in the load train. The axiality and concentricity of the actuator, grips, test specimen, and load cell should be verified and corrected if there is a problem. Coarse adjustments can be made by removing the preload and loosening the load train. These components can then be shifted and/or shimmed to gain proper alignment. Once the load train has been retightened, the small bending strains, *which always exist*, must be measured and minimized. This is typically done by using a strain-gaged trial test specimen, which allows bending strains to be calculated as a function of position along the test specimen, using the same material and test set-up as used in the actual test program. This process can be somewhat involved, and ASTM E 1020 describes it, along with many articles (Ref 22–25).

During axial loading, the bending strains should be kept below a specified amount, as described in various fatigue testing standards. For example, ASTM E 606 recommends that the maximum bending strain should not exceed 5% of the minimum axial strain range used during the test. If the bending strains exceed these amounts, the test rig must be further aligned. In past years, this was done by a trial and error method similar to the coarse adjustment procedure described above. This process could take days of effort to achieve moderate bending results. Recently, a new device has been developed (Fig. 16), which fits into one end of the load train (Fig. 8) and allows adjustment of both angular and concentric components of bending while the load train is under preload. This reduces the time needed for achieving proper alignment to within a few hours.

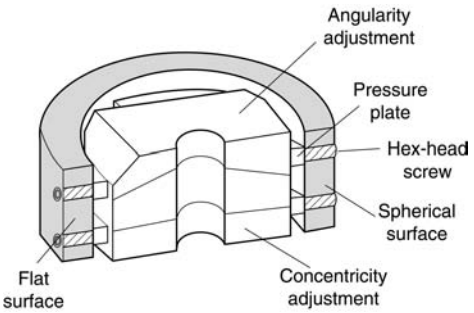

Fig. 16 Alignment fixture for minimizing bending strains in axial fatigue testing

The amount of bending strain in the specimen is affected by gripping methods and specimen design. Better alignment can be achieved using collet, wedge, and button-head grips. Threaded specimens generally give poorer alignment with equally poor reproducibility. Likewise, wear and oxidation of the grips can lead to poor alignment.

Graphic Recorders

In addition to software-based digital recording methods, analog recording devices are also commonly employed for materials testing applications. Strip-chart recorders, enabling time-based paper chart records of various control and response variables, are used. Generally, the strip chart record is used to provide a means to diagnose why a test went off-line, if it does so prior to failure, and to record the gross response variable behavior (e.g., load response) at the point of incipient failure under strain control conditions. Most pen-based strip chart recorders are useful for lower-frequency testing applications (e.g., <1 Hz), because their limited frequency response precludes use to higher frequencies. XY recorders are also commonly employed to record material stress-strain (load-displacement) response or hysteresis loop response in fatigue tests. XY and strip-chart recorders often feature a selection of preset gain ranges (e.g., 0.1 V, 1 V, 10 V or 1 V, 2 V, 5 V, 10 V) for use in plotting signals from the test system. For materials testing applications, it is most desirable that the preset gain controls offer ranges that approximately double the value of the previous setting with each subsequent setting (e.g., 1 V, 2 V, 5 V, 10 V). Analog recorders of these types are often used in conjunction with digital controllers and associated software due to the additional flexibility offered.

Electronic Test Controls

Electronic test controls (controllers) are used to adjust and maintain the desired control parameter(s) for a given fatigue test. Controllers also provide test termination capabilities for many criteria, for example, failure, load drop-off, deflection, or extension limit excellence. Modern fatigue testing is generally performed using closed-loop servocontrollers, wherein the controlled parameter is continually sensed and compared to the desired command, and the result of this comparison, the error signal, is used to drive the actuator (which may be hydraulic or electromechanical in nature). Sensors for measuring the relevant mechanical quantities (e.g., load cells and extensometers, as discussed elsewhere in this article) provide the feedback, and the control mode of the test is defined by the sensor being used for feedback control. Control is typically effected through a PID strategy wherein the error signal is amplified by gain terms that can be independent of time (proportional gain), as well as dependent on time (integral and derivative gain). A typical closed-loop control system is shown in Fig. 17.

A functional fatigue testing machine requires the ability to flexibly define test needs with regard to command waveform generation and data acquisition. A variety of technologies are available to accomplish closed loop control of materials testing systems, in performing standard materials tests, and for the development of custom testing applications. This section discusses these technologies and particularly focuses on the state of the art of software tools for materials testing.

Load Frames: Analog and Digital Controls

Analog controllers are the most commonly used test controllers in fatigue testing laboratories today. Analog controllers have been brought to a high level of refinement, and the latest examples exhibit relatively low noise and reasonably wide-frequency bandwidth. Analog controllers typically provide numerous inputs and outputs that can be used to flexibly adapt to nearly any testing requirement. In addition, materials testing applications software that is designed for analog controllers can be used broadly on many different controller models. The disadvantages of analog controls include the fact that many models do not provide the ability to switch control modes while the test system is energized (under hydraulic pressure), and that calibration of the sensors and the test controller is typically done through trim pot adjustments, a process that can be time consuming.

Digital controllers have been available for the past several years, and the usability of these controllers continues to improve with each new generation. The fundamental difference between an analog controller and a digital controller centers on the summing junction (Fig. 17). A digital controller closes the control loop using a microprocessor instead of continuous-signal analog amplifiers. In a digital controller, the loop closure rate (the rate at which the microprocessor must update the control loop) is directly related to the maximum test frequency performance (i.e., bandwidth) that can be attained. The loop closure rates required for servohydraulic systems demand very-high-performance digital systems. One of the factors driving the development of digital controls is that control mode switching is simpler, as the

loop is digital, and many of the problems relating to offset error in analog systems are not present in their digital counterparts. In addition, from a manufacturer's viewpoint, the cost of digital technology continues to drop (for a given level of performance), and the manufacturing of digitally based products is inherently simpler, owing to fewer required circuit trim adjustments. The chief disadvantages of digital controllers are that changes to the controller organization cannot be done except through software modification of the controller, effectively isolating the user from making any change, and digital controllers generally require software graphical user interfaces. Most digital controller operator interfaces can be labyrinthine to navigate and use, complicating their use and increasing the probability of user mistakes.

Comparison of Analog and Digital Controllers. Both analog and digital control technologies are available for use in performing materials tests, and it is not possible to make definitive statements regarding the superiority of either technology for materials testing needs. The decision as to which controller technology to use may be more prosaic as well: life cycle costs and training costs, among others, must be carefully considered before a choice is rendered. Because analog controllers provide a nearly universal interface for admitting external program command signals, as well as provide high-level conditioned transducer signals for data acquisition, they are easily interfaced to computers for test control purposes. The software created can be generally applied to testing needs regardless of the specific manufacturer's model of the analog servocontroller. Digital controllers, on the other hand, feature software that is based on the "command set" for the specific controller. Thus, materials testing needs that cannot be realized from off-the-shelf software must be custom developed, and any such software is uniquely tied to that specific digital controller model. Finally, analog controllers have a demonstrated longevity, whereas the digital controller will likely have a much more rapid obsolescence, owing to the rapid evolution of digital components.

Furnace Controls

The control of furnaces used in materials testing is largely accomplished using closed-loop temperature controls. Because thermal processes inherently vary slowly (therefore the control loop update rate requirements are relatively modest), and because the costs of microprocessor technology continue to drop, nearly all temperature controllers available today are digitally based. Care must be exercised when selecting a given temperature controller to ensure that it is compatible with the control input requirements of the heating system that is being used. If thermomechanical tests are contemplated, or other nonisothermal temperature requirements are being contemplated, the temperature controller must have facilities for varying the temperature set point, either by means of an external command signal or with a controller command set. Of the two, facilities for accepting an external command signal are preferred, because this provides the greatest flexibility and simplicity in the test apparatus.

Test Program Development and Software

Software systems for performing materials tests have been in use for approximately 25 years (Ref 26). During this period, computer technology has changed dramatically, but, ironically, testing needs have not. Scientists and engineers have a continuing need for flexible and powerful tools to design and conduct materials tests, be they standard tests or unique experiments representative of research and development efforts. Software systems developed to satisfy testing needs have typically been developed along three lines: single application software created uniquely to meet a specific testing requirement (e.g., ASTM E 606), general-purpose testing software designed to provide a flexible set of tools that can be used to implement a broad spectrum of testing requirements, and lastly, custom-written test application software.

Single-Purpose Software. Software for performing standardized tests is widely available from several vendors, operating for both analog and digital servocontrollers. Materials testing engineers charged with conducting standardized materials tests are strongly encouraged to review commercially available offerings before considering custom-application software development. Most specific test requirements (e.g., high-cycle fatigue, low-cycle fatigue, and fatigue crack growth) are well represented by commercially available application software. While the cost of commercial materials testing software is significant, custom-application development is not trivial and is time consuming.

General-Purpose Software. Several examples of general-purpose testing software are readily available from a variety of vendors. Generally, these applications operate on a PC interfaced (in varying degrees of complexity) to a servocontroller, either digital (Ref 27–29) or analog and/or digital (Ref 30–34). These tools permit the construction of reasonably complicated test sequences and provide for data acquisition needs. Some systems provide the ability to build test sequences that are limit programmed (e.g., a load-controlled, strain-limited waveform), can offer multimode test control (e.g., dynamically switching control modes during the test), and can provide the ability to perform calculated control of either or both the control variable, as well as the significant waveform parameters (e.g., amplitude, rate, and frequency) (Fig. 18). Examples of the testing applications that can be accomplished with this class of testing software include TMF, biaxial and multiaxial fatigue, creep-fatigue, and bithermal fatigue. These general-purpose systems have grown in sophistication to the point where one must carefully consider one's testing needs before embarking on a custom-application programming project; often, the general-purpose system can provide the quicker solution and at a much more attractive cost.

Custom-Application Software. When testing requirements are very specific and unique, materials testing engineers must often develop their own materials testing application software. The approach taken can vary widely depending on the nature of the test controller and the needs of the application.

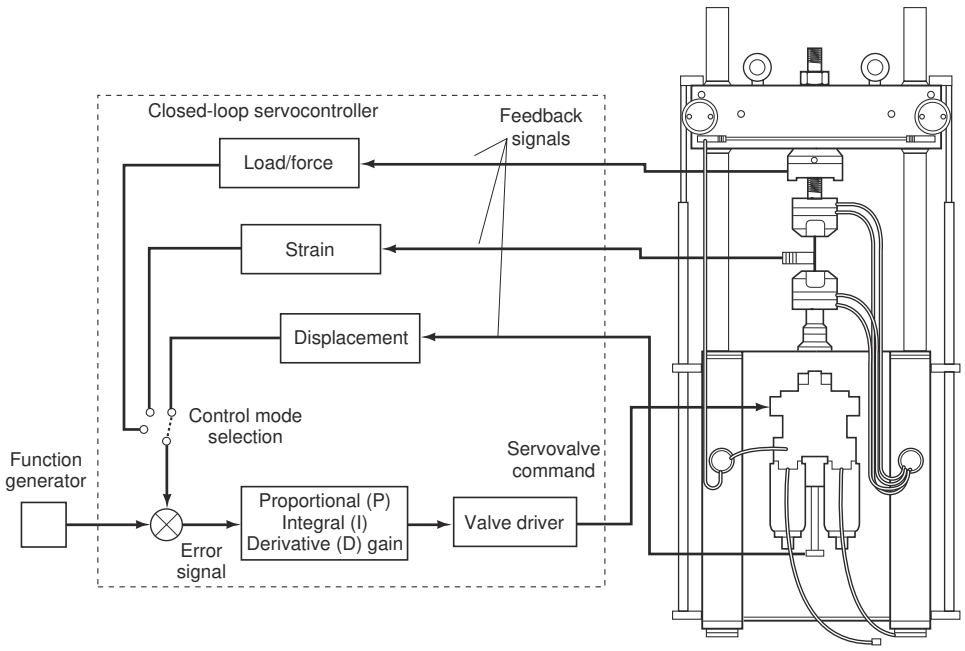

Fig. 17 Typical closed-loop servocontroller system for fatigue testing

Data Acquisition Requirements. Regardless of the approach taken with respect to testing software, certain data acquisition requirements must be met with regard to the amount of data collected, the rate of collection, and the overall accuracy of the data collected. Fatigue tests involving the use of sinusoidal waveforms (commonly used for high-cycle fatigue testing), for example, typically require a data collection rate of fifty points per cycle to enable the cycle to be accurately rendered. A triangular waveform is most often used for low-cycle fatigue testing. Accurately rendering a hysteresis loop in this case requires a data collection rate of up to four hundred points per cycle. When selecting or evaluating data acquisition capabilities for fatigue testing, consideration must also be given to the specific properties of the analog/digital (A/D) system: important characteristics include resolution, accuracy, and noise level. Another important characteristic concerns how the A/D system handles multichannel signal input. Typically, two approaches are taken. The first and most common approach is to simply multiplex the input signals to the A/D system. A concern here is the potential for channel-to-channel data skew: each channel scanned is obtained at a different time than the others. Depending on the conversion rate of the A/D system and the testing frequency being employed, the channel skew can be significant. A second approach for handling multichannel inputs is to use a simultaneous sample and hold amplifier for each channel. In this approach, all channels are sampled and held at the same time and are then multiplexed to the A/D for conversion. Yet other data acquisition systems employ individual A/D converters for each input channel (see ASTM E 1856 for a more detailed discussion of this topic).

Data Analysis. The software available for data analysis largely mirrors that available for testing applications; the standardized test applications generally have built-in data analysis and reporting capabilities, optimized to report test results in standardized formats. However, test data obtained from general-purpose testing software, and especially data obtained from custom-application programs, must generally be imported into a data analysis program. The most common data analysis programs are the scientific data analysis and plotting applications widely available from many vendors. Another popular method is to import test data into spreadsheet programs. Many of the scientific analysis packages (as well as the spreadsheet programs) provide the ability to develop reasonably sophisticated analysis algorithms ("macros" in spreadsheets, for example), thus providing a convenient and powerful means of data analysis and presentation.

Baseline Isothermal Fatigue Testing

It is important to understand the underlying purposes of the testing to be performed. This understanding will aid in selecting a fatigue testing machine and specimen design. Normally, a baseline condition is established from which effects on fatigue life of a wide variety of variables might be assessed. Laboratory ambient conditions of room temperature, atmospheric pressure, and humidity are a commonly accepted condition for baseline testing; however, other choices of, for instance, temperature may be more appropriate. Baseline testing is usually performed with the numerous fatigue life-influencing variables held constant at what would be considered "default" conditions. For example, completely reversed loading (zero mean stress) may be used, or perhaps zero-to-maximum loading is preferred owing to the nominal zero-to-maximum loadings expected in service. Note that rotating-beam machines are incapable of mechanically imposing mean stresses. If mean stress assessment is contemplated for testing beyond the baseline, a different type fatigue machine is required.

The acquired baseline database may have value in serving any of several diverse purposes:

- Ranking fatigue resistance of alloys
- Performing micromechanistic studies
- Guiding development of fatigue-life prediction models
- Collecting statistical documentation
- Establishing fatigue design curves
- Conducting failure analysis

Testing Regime. Of additional importance is the fatigue-life regime of interest—low-cycle or high-cycle fatigue. As discussed earlier, the amount of time available for testing, along with the number of companion machines and their cyclic frequency capability, will dictate which type of machine is best suited for the task at hand. For fatigue lives far beyond 10^5, a high frequency of testing is a necessity. However, at lives well below 10^5, high frequency is a liability, not an asset. With the exception of very high cyclic lives, servohydraulic direct-stress

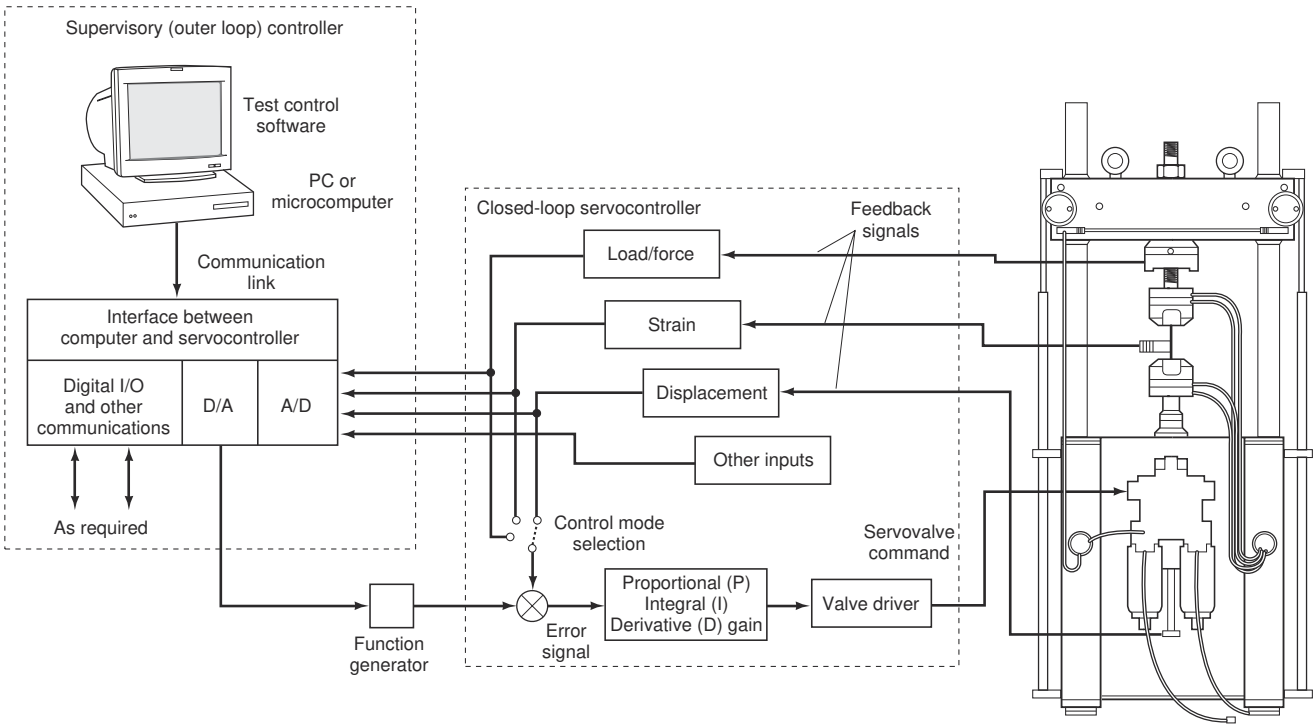

Fig. 18 Typical supervisory (outer loop) calculated-variable controller system for fatigue testing

testing machines offer the greatest possible versatility in testing machines today. Specially designed, and hence costly, commercially available servohydraulic machines can achieve 1000 Hz.

Calibration and Standard Test Procedures. Once equipped with an appropriate fatigue testing machine and a specimen design, it is important to follow applicable standards for testing (e.g., ASTM and ISO standards). The major items covered by ASTM standards include calibration of, for example, load cells, extensometers, other sensors, read-out equipment, and recorders for data storage; alignment of the loading axis of the testing machine with grips and with the test specimen; specimen design, including alignment of the test section with grip ends; surface finish; material quality control from specimen to specimen; and purity of loading command signals. Table 1 lists the currently applicable ASTM standards for baseline (and associated) fatigue testing.

Adhering to testing standards is particularly important in fatigue testing due to the inherently high degree of scatter in fatigue resistance. In creating the standards, efforts were made to ensure uniformity of specimen geometry, surface finish, loading alignment and gripping, temperature and humidity (for alloys sensitive to moisture level), and uniformity in all aspects of the testing machine frame and loading train, its ancillary equipment, controllers, recorders, data storage, and data manipulation.

Generating Fatigue Crack Initiation Data. The loading mode, life regime, test temperature and environmental conditions, mean stress, surface finish, and heat treatment condition, among others, dictate the testing machine and ancillary equipment required. Once these are in place and calibrated and the representative test specimens have been prepared, a baseline fatigue testing program can be conducted. If the program involves several variables, it is wise to first perform a design-of-experiments study to maximize the information to be obtained while minimizing the number of tests and attendant costs. In any event, it should be noted that the cost of specimen preparation is usually not the dominant cost in a fatigue testing program. It is wise to ensure that a sufficient excess of specimens is made to more than adequately cover the initial number required in the program. Having specimens left over from a baseline study is often beneficial, particularly if additional factors are to be studied and if scatter in fatigue lives has been great enough to warrant additional tests to better establish the statistical results. It is generally not possible to duplicate the specimen consistency at a much later date, so it is better to have extra, rather than not enough, specimens to begin a test program.

It is advisable to estimate the expected fatigue life of any test prior to starting the test to avoid excessively long or short test times. Past testing experience with similar materials is valuable in making life estimates. Empirical equations have been published for estimating fatigue resistance based on conventional tensile test data for the material, temperature, and environment of interest. The equations of Manson (Ref 35) and Morrow (Ref 36) have proven invaluable in this regard (see Eq 1, which follows). In fact, the method of universal slopes (MUS) has been used to bypass fatigue testing (Ref 35). With appropriate factors of safety, the MUS has been used in the establishment of low-cycle fatigue design curves for many of the alloys used in the main engines of the US space shuttle (Ref 37). The fatigue resistance of a large number of alloys in a variety of heat-treated conditions over a range of temperatures and aggressive environments has been established in this manner.

If a broad range of testing times are to be involved, it is also advisable to conduct the shortest-time tests first, then take advantage of these results to govern the loading levels applied for the longest-life tests. One should avoid running tests that must be discontinued. Considerably less information is gained from such "run-outs."

Sufficient tests should be run to failure over the range of variables studied to permit a statistical assessment of the results. This is particularly true for the baseline results from which other fatigue test results are to be compared.

The extent to which the test data are recorded *during testing* depends on the end use of the fatigue data. In high-cycle fatigue, most alloys behave nominally elastically, and there is little reason to monitor test parameters during the test, as there will be little (if any) change to observe until fatigue failure is imminent. However, in strain-controlled low-cycle fatigue with observable amounts of plasticity, significant changes might occur that warrant recording, for example, cyclic strain hardening or softening, relaxation of mean stress, and even cyclic stress-strain response changes due to crack nucleation. It is quite important to be able to monitor these changes during testing. For example, the hysteresis loop at "half-life" is usually chosen to be the representative loop of the entire fatigue test. This loop provides the values of the stress amplitude, stress range, mean stress, total strain range, inelastic (plastic) strain range, and the elastic strain range that are tabulated along with the number of cycles to failure. Since the number of cycles to failure is not known until after the test has passed the half-life point, it is necessary to monitor and record this information either continuously or at intervals close enough to be able to interpolate to the half-life condition once the test has failed.

Baseline fatigue data are generally tabulated and plotted. Schematic fatigue curves (Ref 38) are shown in Fig. 19(a) for strong, tough, and ductile alloys. The corresponding stress-strain hysteresis loops are depicted in Fig. 19(b). This figure illustrates the common observation that the number of cycles to failure for a 1.0% total strain range is approximately 1000 cycles, regardless of the strength or ductility level of an alloy when there is a trade-off between strength and ductility due to different alloy processing. Presuming an equation form, fatigue data can be analyzed using least-squares curve-fitting analyses. The most common equation form for low-cycle fatigue and for lives to about 10^6 cycles is:

$$\Delta\varepsilon_{total} = \Delta\varepsilon_{elastic} + \Delta\varepsilon_{plastic} = B(N_f)^b + C(N_f)^c \quad \text{(Eq 1)}$$

where, $\Delta\varepsilon_{total}$ is the total mechanical strain range at half-life, $\Delta\varepsilon_{elastic}$ is the elastic strain range (equal to $\Delta\sigma/E$) at half-life, $\Delta\varepsilon_{plastic}$ is the plastic (inelastic) strain range at half-life, N_f is the number of cycles to failure, b is the slope of elastic strain-range life line on log-log coordinates, B is the intercept of elastic strain-range life line at $N_f = 1$, c is the slope of plastic strain-range life line on log-log coordinates, C is the intercept of plastic strain range life line at $N_f = 1$, $\Delta\sigma$ is the stress range at half-life, and E is the modulus of elasticity. The method of universal slopes that is used to estimate fatigue curves has the same form as Eq 1. The values of the "universalized slopes" are given by $b = -0.12$ and $c = -0.60$.

The corresponding values of the intercepts are determined from conventional tensile test results for the alloy at the temperature and environmental conditions of interest: $B = 3.5\sigma_{ult}/E$ and σ_{ult} is the ultimate tensile strength, and $C = D^{0.6}$. True ductility (also true fracture strain) is abbreviated D; reduction of area in the tensile test is abbreviated RA.

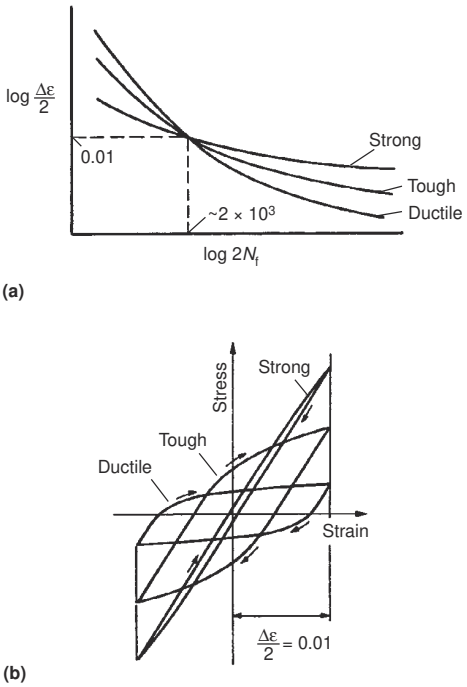

Fig. 19 Representation of the cyclic strain resistance of idealized alloys (strong, tough, ductile). (a) Fatigue curves. (b) Stress-strain hysteresis loops. After Ref 38

$$D = \ln[(100)/(100 - \%RA)]$$

Morrow's formulation is similar and has seen widespread use in the automotive and off-highway equipment industries. It takes the following specific form:

$$(\Delta\varepsilon_{total}/2) = (\Delta\varepsilon_{elastic}/2) + (\Delta\varepsilon_{plastic}/2) = (\sigma'_f/E)(2N_f)^b + \varepsilon'_f(2N_f)^c \quad \text{(Eq 2)}$$

where $\Delta\varepsilon_{total}/2$ is the total mechanical strain amplitude at half-life, $\Delta\varepsilon_{elastic}/2$ is the elastic strain amplitude ($\Delta\sigma/2E$) at half-life, $\Delta\varepsilon_{plastic}/2$ is the plastic (inelastic) strain amplitude at half-life, $2N_f$ is the number of reversals to failure ($2 \times N_f$), b is the slope of the elastic strain-amplitude life line on log-log coordinates, σ'_f/E is the intercept of elastic strain amplitude life line at $2N_f = 1$, c is the slope of the plastic strain-amplitude life line on log-log coordinates, ε'_f is the intercept of plastic strain amplitude life line at $2N_f = 1$, and $\Delta\sigma/2$ is the stress amplitude at half-life.

Morrow's fatigue-life equation in its predictive form assumes the slopes and intercepts can be approximated from tensile test properties by $b = n/(5 + n)$, where n is the strain hardening exponent (the cyclic strain hardening exponent, n', may give better predictions; $n' = b/c$; $c = 1/(5 + n)$; and $\sigma'_f/E = \sigma_f/E$, where σ_f is the true fracture stress (fracture load divided by fracture area). The true fracture strain is equal to the true ductility, D, is equal to ε'_f is equal to ε_f.

The slopes and intercepts from the equations above are referred to as the basic fatigue properties. Reference 39 contains an extensive listing of these fatigue properties, along with corresponding tensile properties, for a wide variety of steels, stainless steels, nickel-base superalloys, titanium alloys, aluminum alloys, weldments, and castings. How the fatigue properties might be affected by factors that influence fatigue behavior is discussed in the section "Testing for Effects of Variables on Fatigue Resistance" in this article.

In the high-cycle fatigue regime, that is, beyond approximately 10^6 cycles to failure, the log-log slopes of the fatigue curves tend to become shallower than at lower life levels. For certain steels and selected body-centered cubic (bcc) alloys, a fatigue or endurance limit of "infinite" life for cyclic stresses below the limit may be observed in laboratory fatigue test results. Such limits may be erased by interspersed low-cycle fatigue loadings that can break up the dislocation pinning by small interstitial atoms in the bcc structure. Under these circumstances, the fatigue curve continues to drop in strength level below the original fatigue limit. Slopes of the fatigue curve in the very-high-cycle fatigue regime may drop to –0.04 or less. Manson (Ref 40) has reported ultrahigh-cycle fatigue life extrapolation procedures.

Criteria for Defining Fatigue Life. The first and most common definition of fatigue life for alloy testing is the number of cycles of loading required for complete fracture of the specimen into two pieces. This definition is unequivocal. It is easy to identify this terminal event in most fatigue tests. (During strain-controlled tests at low strain amplitudes, cracking may reduce the stress level sufficiently so that the specimen never separates; in this case, some other definition of failure must be used.) At fracture, the specimen grips are free to move apart, allowing a mechanically activated switch to be tripped that stops the cyclic drive mechanism and the cycle counter. Electrical continuity of the specimen is also broken permitting direct electrical switching of circuits controlling the machine. Complete specimen separation is typically an acceptable measure of the crack initiation fatigue life for high-cycle fatigue wherein the fatigue crack nucleation portion dominates the total life (perhaps 90–99%). However, because the separation life does include a portion of cyclic crack growth, this quoted life is somewhat larger than the number of cycles to physically initiate a crack. As the fatigue loading levels increase and the cyclic lifetime decreases into the low-cycle fatigue regime, less and less of the life is spent nucleating a crack, and more and more life is spent growing the crack(s) to the critical length for sudden fracture into two pieces. To accurately define the cyclic crack initiation life, particularly in low-cycle fatigue, one ideally would measure the actual crack size (depth and length) as cycling progressed. When a predetermined crack size was reached, the number of cycles to "failure" would be noted and testing stopped. Unfortunately, this is highly impractical for most testing because it cannot be implemented on an automated basis for the large numbers of fatigue tests conducted annually.

The only practical definitions available are those based on measurements that are readily available from the test instrumentation. This is usually in the form of changes in specimen elastic or plastic "stiffness" as determined from stress-strain or load-deflection measurements. As a specimen develops a fatigue crack under completely reversed strain control, its growth causes the load carrying response of the specimen to decrease. Different degrees of drop in the cyclic load range for a fixed strain range have been used to define crack initiation failure for low-cycle fatigue testing. The most commonly used criteria have been the very first indications of an impending drop in the load range (i.e., impending cracking) and a 5% drop in the load range. Obviously other percentage drops (10, 20, and 50) could be defined and used. Unfortunately, it may be difficult to distinguish between load range drop due to cracking and load range drop due to cyclic strain softening of initially work hardened materials. Even cyclic strain hardening could confound the measurement by offsetting the drop due to cracking.

A logical way to separate the effects on load response of cyclic strain hardening or softening from cracking is to track the ratio of the peak tensile load to the peak compressive load (Ref 41). If only hardening or softening occurs, the load range will change, but the tensile/compressive load ratio will be affected very little. As fatigue cracking progresses, the decrease in the tensile load amplitude exceeds that of the decrease of the compressive load amplitude. This is observable in Fig. 20(a) from a load-versus-time trace for a low-cycle, completely reversed, strain-controlled test (Ref 42). As cracking occurs, the change of the load ratio is almost twice as much as the change in the load range, thus making it a more sensitive, as well as a more physically based, measure of cracking. The load response would also be observable in a stress-strain hysteresis loop. In compression, the crack faces close and carry load. This results in a cusp on the hysteresis loop near the compressive peak. In tension, the peak load is carried only by the smaller, uncracked area.

To apply these criteria for defining fatigue crack initiation life, the load ratio must be measured during the precrack nucleation period. Note that the load ratio during this interval may not equal 1.00. It has been observed to vary from as low as 0.9 to about 1.05 depending on material. The ratio, however, is nominally independent of the amount of cyclic hardening or softening that occurs, and, hence, a greater duration of cyclic loading can be used to establish the average value of the ratio before cracking commences. A graphic quantitative example is given by Fig. 20(b) based on the data from Fig. 20(a). Both load ratio and load range are plotted versus applied cycles. The load ratio is relatively constant at 0.96 for the first half of the test, but, by about 100 cycles, it begins to drop steadily. At about 200 cycles, the ratio suddenly and inexplicably rises. This rise signals the end of useful information from the test. Even though the specimen is still in one piece, the computed stresses and strains are no longer representative of what is going on in the gage length of the specimen. At this point, the dominant crack has grown to a large fraction of the specimen diameter, and the extensometer is subjected to large amounts of bending in addition to axial deformation. The specimen may not have failed completely, but the test has. The corresponding load range is also shown. After considerable initial hardening of 25%, a half-life ("stabilized") value of 2800 lbf (12.5 kN) is reached. This is followed by an accelerating drop until complete fracture of the specimen occurs at greater than 214 cycles. For the particular test data shown, the load ratio and the load range follow approximately parallel behavior. For this example, a 5% drop in load range and load ratio corresponds to the same number of cycles (~138 cycles). Similarly, a 10% drop in both gives approximately 158 cycles. In this case, either the load range or the load ratio drop criteria would give acceptable definitions of fatigue crack initiation life. This is not expected to be the general case for the following reasons.

For a cyclically stable material with very little strain hardening within a hysteresis loop, a

5% load range drop would correspond to approximately a 10% drop in the load ratio if the only reason for load drop were the presence of a crack. This in turn would imply a 10% loss in specimen cross-sectional area if there were no concentration of stress surrounding the crack tip. However, since there is a concentration of stress in front of the crack, higher stresses are encountered there, thus increasing the tensile load-carrying capacity. Hence, a 10% loss of area would actually correspond to less than a 10% loss of load ratio. Load ratios in the neighborhood of 5 to 8% have been noted.

With modern automated data recording and reduction, it is possible to determine the fatigue life by all of these definitions, including complete fracture into two pieces. In this way, any definition of fatigue crack initiation life can be selected for the purposes at hand. References 41 and 42 contain tabulated fatigue crack initiation lives for several engineering alloys for the four criteria, as discussed above:

N_0	First indication of impending cracking
N_5	5% drop in load range from stabilized range (or at half-life value if stabilization does not occur)
N_i	10% drop in ratio of tensile to compressive load from stabilized range (or at half-life if stabilization does not occur)
N_f	Complete separation of specimen

Similar criteria based on the same concepts could be established for completely reversed, load-controlled tests. Instead of a decrease in load response due to cracking, an increase in strain or deflection response would be measured to define fatigue crack initiation.

Care should be exercised in applying these criteria when multiple cracks initiate parallel to one another. Many shallow cracks will have the same integrated effect on specimen gage length compliance as one deeper crack. In addition, the exact location of the crack(s) relative to the contact points (defining the gage length) of the extensometer can have an appreciable influence on the apparent (measured) compliance. For example, should cracking initiate outside the gage section, the extensometer would not detect a change in compliance. Should cracking initiate within the gage section, the load path would not necessarily remain along the centerline of the specimen, and bending would occur. This, in turn, can cause the extensometer to register different outputs depending on the plane of bending relative to orientation of the extensometer. These confounding influences also affect the load range drop criteria for crack initiation.

Information to be Documented for Baseline Fatigue Tests. Guidelines are presented for what baseline fatigue test information should be documented. Tables 2 and 3, respectively, provide comprehensive listings of pertinent pretest and in-test/post-test information to be considered for inclusion. In preparing Table 3, it was assumed that closed-loop; servostrain-controlled axial fatigue testing was the mode of operation. If other modes of testing are used, the guidelines may have to be altered accordingly. Obviously, the information gleaned from a fatigue test in progress will depend on the

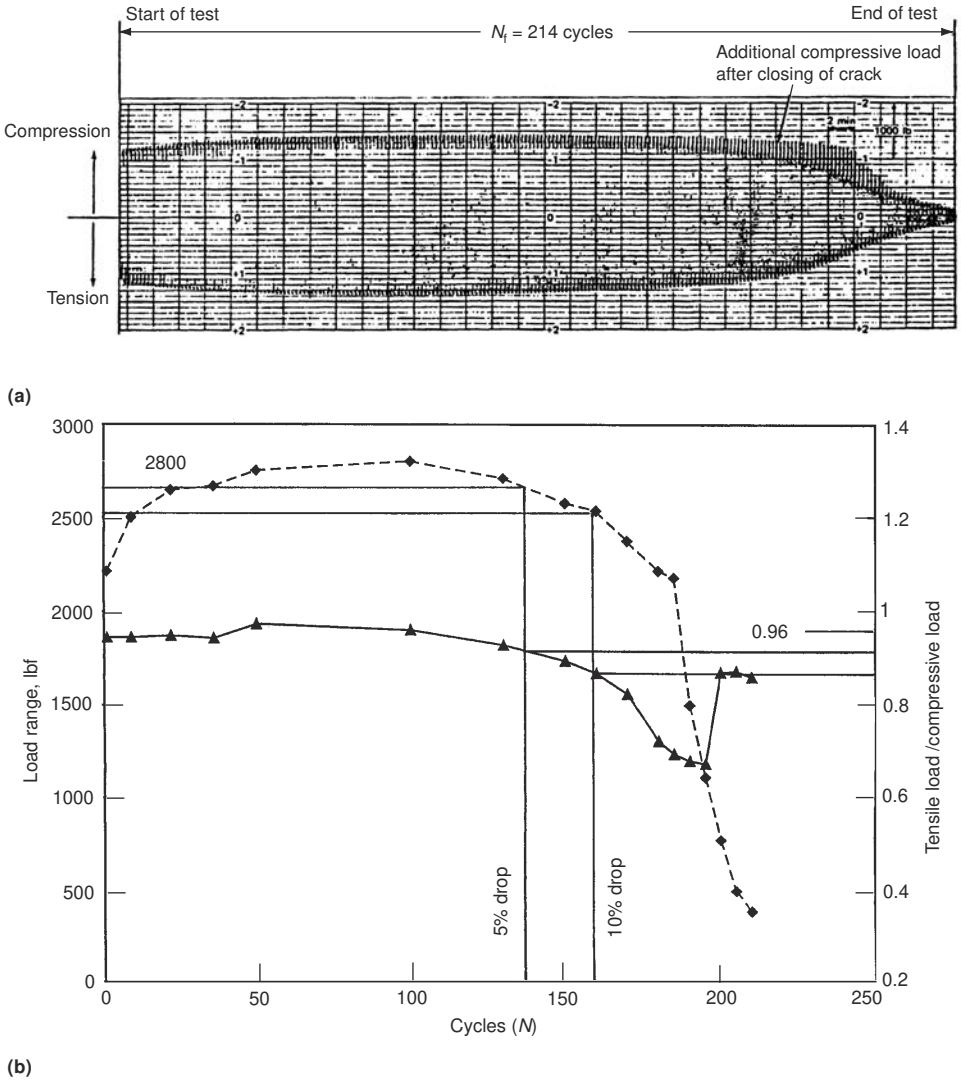

Fig. 20 Cyclic load response during strain-controlled low-cycle fatigue test of annealed AISI 304 stainless steel in air at 816 °C (1500 °F). Total strain range, 3.26%, 0.056 Hz. (a) Cyclic load response for defining cyclic life to crack initiation. (b) Cyclic load range and ratio of tensile to compressive peak load versus applied cycles. Source: Ref 42

Table 2 Pretest information guidelines for baseline fatigue tests including studies of preexisting effects on fatigue

Alloy designation and description	Heat number and composition, forming processes, degree of anisotropy, heat treatment and environmental preexposure conditions, final machining parameters, photomicrographs, hardness, tensile properties
Specimen configuration	Drawing and specifications, orientation of axis to product form, accurately measured specimen dimensions (including notch description) and area of cross section (diameter and area for direct stress mode of loading), surface finish and method of preparation, final heat treatment, individual specimen identification number, description of any coatings including any processing affecting the surface layer (preoxidation, prefretting, galling, wear, erosion, corrosion, carburizing, nitriding, anodizing, shot peening, laser-shock peening, burnishing, and other means of introducing residual stresses, magnitude, and sign of residual stresses, etc.), thickness, orientation of gripped specimen to testing machine
Testing machine	Designation of machine, type of grips, dates of last alignment and calibration of load cell, types of heating and environmental control, type of extensometer, and date of last calibration
Test engineer and operator	Names and dates of set-up and start of test
Testing mode, control details, and test conditions	Model of control (e.g.,strain, load, or deflection), cyclic frequency and waveform including description of mean and alternating components, test temperature and means of measurement and control, relative humidity and nature of environment, starting date and time, error detector limits for shut-down, estimate of test duration and basis for estimate

extent of instrumentation available, the type of testing machine, and the mode of testing.

Example Crack Initiation Fatigue-Life Curves. Fatigue curves are displayed in a variety of forms, although fatigue life is generally plotted on a logarithmic scale. The fatigue loading parameter is usually stress or strain. Stress is most commonly plotted as stress amplitude, stress range, or maximum stress, and the scale may be arithmetic or logarithmic. Examples are given in Fig. 21. These are referred to as *S-N* curves, and an indication of the mean stress ratio should always be given. When strain is the fatigue loading parameter, the total (elastic plus plastic), plastic, or the elastic strain ranges may be plotted. These are usually plotted on logarithmic scales, as shown in Fig. 22, and are referred to as strain-life curves. Unless the fatigue strain cycling ratio is given, it is understood that the curves represent completely reversed loading. The plastic strain-versus-life curve is known as the Manson-Coffin (or Coffin-Manson) low-cycle fatigue curve. The elastic strain range-versus-life curve has come to be known as the Basquin curve (Ref 43). The total strain range-versus-life representation of fatigue data has its origins in the late 1950s and early 1960s. Coffin (Ref 44) originally represented the elastic strain range-versus-life component of the total strain range-versus-life curve as a horizontal line with a strain range value equal to twice the 0.2% offset yield strength divided by the elastic modulus. Langer (Ref 45) used the same basic idea, but replaced the yield strength with the endurance limit strength. He went on to multiply the total strain amplitude by the modulus of elasticity to compute the pseudo-stress amplitude. The resultant fatigue (*S-N*) curve could then be used in direct conjunction with elastic stress analyses. This representation was adopted by the ASME Code, Section III, for Boiler and Pressure Vessel components.

Manson (Ref 46) and Morrow (Ref 36) carried the fatigue curve representation a step further by recognizing that the elastic strain range-versus-life curve had a negative slope such as first observed by Basquin a half century earlier.

Out of the total strain range-versus-life representation of fatigue resistance comes an important observation and useful concept (e.g., see Ref 40). At some point along the fatigue curve, the elastic strain range and the plastic strain range will be equal. This point defines what is known as the transition fatigue life, $N_{f,trans}$, and the corresponding transition total strain range, $\Delta\varepsilon_{total,trans}$, is equal to $2\Delta\varepsilon_{plastic}$, which is equal to $2\Delta\varepsilon_{elastic}$. Below the transition fatigue life, the behavior is clearly low-cycle fatigue as the plastic strain range dominates over the elastic strain range. Low cycle fatigue actually continues to higher lives beyond the transition life. High-cycle fatigue behavior, in which the elastic strain range overwhelmingly dominates over the plastic strain range, does not begin until at least one order of magnitude in life beyond the transition life.

Table 3 In-test and post-test information guidelines for baseline fatigue tests including studies of preexisting effects on fatigue

Cyclically varying parameters	Value of fixed test control parameters (e.g., stress, strain, or displacement); continuous recording of variations of maximum, minimum, amplitude, range, and mean values of stress and strain as a function of applied cycles; cyclic variation of load range variation and ratio of tensile to compressive peak loads to help define failure life and half-life; continuous or periodic recording of variations of stress-strain hysteresis loops
Lifetime information	Cyclic failure lives based on various cyclic failure criteria; failure life (cycles and corresponding time) for criterion adopted; half-life cycles; total, inelastic, and elastic strain ranges at half-life; maximum, minimum, stress amplitude, stress range, mean stress, and mean stress ratio at half-life; degree of cyclic hardening and/or softening from first cycle to half-life (or cycles at stabilization of stress-strain response); description of fracture surface including initiation site(s); location of fracture relative to extensometer probes
Deviations from original test plans	Details of stress and strain history immediately prior to controlled or uncontrolled shut-downs prior to test completion
Data analysis from multiple specimens	Cyclic stress-strain curve and equation constants at half-life (or cycles at stabilization), fatigue curves and equation constants (i.e., fatigue properties)

Testing for Effects of Variables on Fatigue Resistance

The fatigue resistance of an alloy is sensitive to a large number of variables. There are too many variables to investigate them all. To do so would require an enormous test matrix, a large number of fatigue testing machines, and a huge

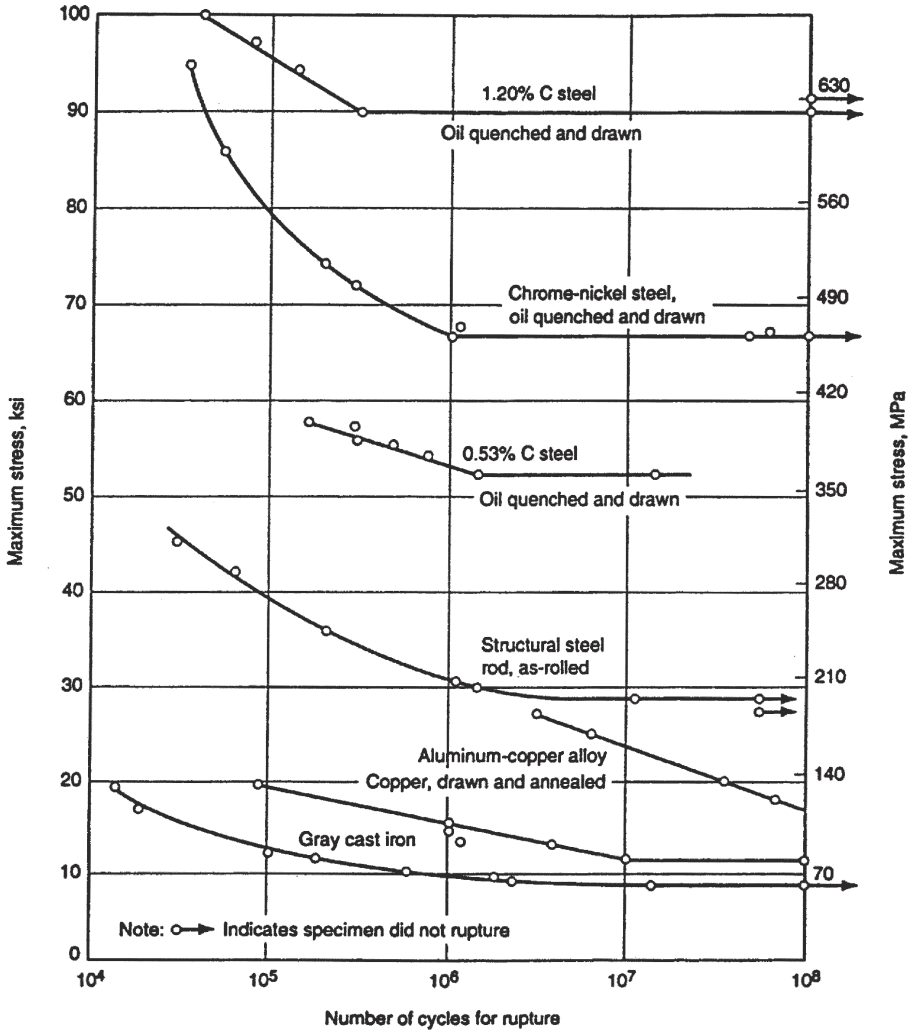

Fig. 21 Typical *S-N* diagrams for various alloys subjected to completely reversed loading at ambient temperature

budget. Fortunately, similar behavior trends are observed by various classes of alloys. This allows engineers to experimentally document the behavior of many of the more commonly encountered variables using only a limited number of tests. As a prime example, several different models can describe the effects of mean stress on fatigue life. All predict lowered fatigue resistance to tensile mean stress and enhanced life with compressive mean stress. Another example is the correlation between tensile test properties and baseline fatigue resistance as given by Eq 1 and 2, that is, increases in the ductility of an alloy generally enhance low-cycle fatigue life, whereas increases in tensile strength produce greater high-cycle fatigue resistance. These correlations have proven quite valuable. If more accurate assessments of the effects of variables on fatigue are required, they can be determined experimentally. This section discusses the more commonly investigated variables.

The variables affecting fatigue can be categorized into four types: bulk and geometric factors, and surface- and active loading-related factors. Common examples of each type are listed in Table 4. Synergistic interactions may occur among these influences. For example, the loading-related factor of high-temperature testing in air would induce the surface related factor of oxidation. Seldom are surface-related effects of this nature beneficial to fatigue resistance.

Bulk and surface-related property effects could be further classified as preexisting or concurrent. Geometric effects are generally preexisting with respect to laboratory specimen fatigue testing. Examples of preexisting bulk effects are cold working introduced during the forming process and metallurgical heat treatment of the alloy. Either could significantly alter the strength of an alloy and, hence, alter its fatigue resistance. Concurrent effects can include time-dependent creep, oxidation, or solid-state metallurgical changes, all resulting from exposure of the alloy to high temperature during operational use or specimen testing. Effects on fatigue resistance of preexisting factors can be dealt with by simply considering the alloy as a new material to be evaluated.

Concurrent influences, however, require additional consideration to ensure testing adequately reflects the influences encountered in service. For example, high-temperature service may involve more than an order of magnitude greater exposure time than can be afforded during fatigue testing. Consequently, the testing program must be designed to provide data that can be extrapolated with confidence into the time regime of practical interest. This is a particularly vexing problem in the area of high-temperature fatigue, creep-fatigue, and TMF testing of alloys.

Invariably, engineering models of fatigue behavior are created to allow confident interpolation and extrapolation, particularly for structural applications. Models are calibrated to reflect the influences of a multitude of variables. Many models have been proposed over the past century. Those of greatest value for engineering design are the ones that are relatively simple, logical, and clearly reflect a cause-and-effect relationship. They are the easiest to remember and use. Those models that reflect a high degree of mechanistic fidelity are naturally of greatest benefit to the material science and failure analysis community. If such models can also be expressed in tractable terms, engineers will also use them for designing in structural durability of machine components. Understanding the root causes of fatigue permits engineers to better guard against this insidious failure mode.

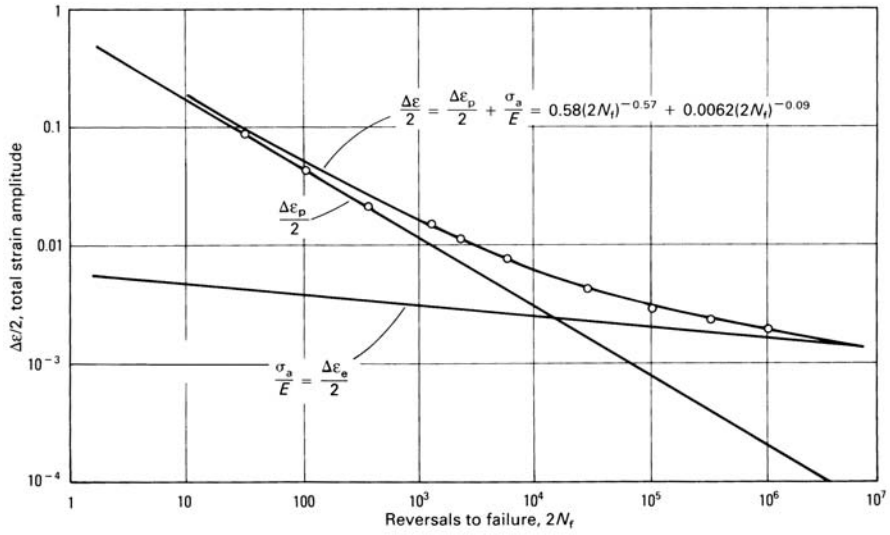

Fig. 22 Typical strain-life fatigue curve showing elastic and plastic components, annealed 4340 steel

Table 4 Significant variables affecting fatigue resistance

Bulk property effects	Degree of cold working and/or annealing
	Heat treatment
	Anisotropy (forming, directional solidification, or single crystal)
	Alloy composition
	Nuclear radiation
Surface-related effects	Mechanical surface finish (e.g., as-cast, forged, machined, or ground)
	Residual stresses
	Mechanically induced (e.g., shot peening, burnishing, laser shock peening; machining, or grinding)
	Thermally assisted (e.g., rapid surface solidification, welding, electrodischarge machining, carburizing, or nitriding)
	Environment (oxidation, sulfidation, corrosion, ion transport, or hydrogen embrittlement)
	Cavitation
	Fretting and galling
	Wear and erosion
	Coatings (plating, anodizing, ion implantation, oxidation protective, or thermal barriers)
Geometric effects	Notches
	Edges and thin sections
	Size effects and highly stressed volume
Active loading-related effects	Actively imposed mean stresses and strains
	Multiaxiality of stress and strain (proportional and nonproportional)
	Cumulative damage (variable levels and types of loading)
	Temperature of testing (from cryogenic to high)
	Creep-fatigue interaction (low frequency, low strain rate, stress hold times, strain hold, and tensile-versus-compressive hold times)
	Thermal fatigue, TMF (continuous temperature strain cycling and bithermal cycling)

Preexisting Variables

Because of the similarities of testing for preexisting bulk or surface-related effects on fatigue resistance, they will be discussed together. Guidelines for information to be documented from fatigue tests of preexisting variables are contained in Tables 2 and 3.

Bulk Property and Surface-Related Effects. Material with preexisting effects can be evaluated by conducting fatigue tests using the same techniques and procedures as for baseline fatigue testing. The affected material is considered as a new material, but one for which some background knowledge exists. It is not uncommon to see a series of fatigue curves for the same alloy composition wherein each curve reflects differing degrees of cold working, heat treatment, or surface finish. The fatigue results

are typically used to select an optimum fabrication method or to indicate material conditions to be avoided. In general, fewer fatigue tests are required, *provided the baseline results are well behaved and well defined.* However, if there were more scatter in the property-affected results, more tests would be required to adequately define the new fatigue curve.

Geometric Effects. The most commonly investigated geometric effects are those of notches and the degree of the theoretical stress concentration, K_t, they impose. Invariably, the fatigue resistance decreases with higher stress concentration factors. The extent of fatigue strength loss for a given fatigue life, however, is never as great as might be suggested by the value of the stress concentration factor. Furthermore, the effectiveness of the stress concentration factor decreases as the root radius decreases and the overall size of the notch decreases. There are several reasons for this behavior that are adequately explained in most textbooks covering fatigue. As discussed earlier, it is of great importance to fatigue testing that uniformity of the notched specimens be maintained to reduce confounding scatter issues. Particular care is required to achieve this goal when dealing with very small notch root radii.

The testing of notched specimens in the high-strain, low-cycle fatigue regime may introduce yielding at the root of the notch. If the cyclic loads are great enough, the yielding will occur on each cycle, despite the fact that the overall specimen appears to behave nearly elastically. The cyclic strain range at the notch root will be larger than indicated by the theoretical stress concentration factor, and the cyclic stress range will be smaller. Analytic approaches are available to describe the stress-strain behavior at the notch root in terms of the applied loading and the cyclic stress-strain curve of the material. See, for example, applications (Ref 47, 48) of Neuber's (Ref 49) and Glinka's (Ref 50) notch analysis approaches. Also of great importance to the fatigue testing of notched specimens is the cyclic relaxation of initial mean stresses at the notch root. For example, for zero to maximum load-controlled cycling, the local notch root stress can relax from an initial zero to maximum condition on the first cycle to a completely reversed condition as cycling progresses. Such changes in the local stress-strain response have a profound influence on the fatigue life of notched specimens. As the cyclic loading level is decreased and longer lives are achieved, there is less and less of a chance for relaxation of the initial cycle mean stress. Consequently, the resultant fatigue curve will exhibit a very low mean stress effect in the low-cycle regime, but will exhibit the full effect of mean stress in the high-cycle regime. Without performing a local stress-strain analysis at the root of the notch, it is nearly impossible to ascertain whether or not a mean stress will relax, and to what extent. The issue of mean stress relaxation becomes critically important in performing cumulative fatigue damage experiments with notched specimens.

Other specimen geometric effects include thin sections and sharp edges. Both can result in fatigue-life reductions due to the fact that there is far less constraint to the motion of dislocations due to the high ratio of surface area to volume. This effect is accentuated at high temperatures wherein creep can occur more readily by grain boundary sliding. Reducing a section thickness to only one or two grain diameters can greatly reduce the normal constraint offered by surrounding grains, thus enhancing creep deformation and increasing the degree of creep-fatigue interaction. When performing fatigue, creep-fatigue, and TMF tests of thin sections, one should caution against having too few grains through the thickness.

Yet another preexisting geometric aspect is the so-called size effect. The smaller the volume and related surface area are for the fatigue-affected zone of a test specimen, the less probability there is of encountering a microscopic flaw leading to early crack initiation. Large specimens with relatively large volumes and high surface areas will invariable exhibit lower fatigue lives than small specimens with relatively small volumes of highly stressed material. While this effect is not an overwhelming one, it should be considered when selecting a particular fatigue specimen for a testing program. In general, the highly stressed volume should be as large as can be tolerated, because many practical machine components have much larger highly stressed volumes than can be accommodated in a corresponding fatigue test specimen.

Concurrent Variables

Concurrent changes of the variables affecting the fatigue resistance are obviously more complex to evaluate. The fatigue resistance being measured is a moving target and quantitatively depends on how much change has accrued over the period of testing. Concurrent changes are due to bulk and surface-related factors, as well as active load-related effects due to mechanical loading and temperature changes during testing. Obviously, the information to be documented for fatigue tests involving concurrent variables is more extensive than shown in Tables 2 and 3.

Bulk Property and Surface-Related Effects. Keep in mind that the laboratory fatigue results are being measured to help assess the structural durability of hardware with specific missions of exposure, loading, temperature, and time, among other factors. Mission loadings often have total durations lasting into years of exposure that cannot be affordably duplicated in laboratory tests. The laboratory coupon results must, therefore, capture the concurrent influences in such a way that they can be generalized and then brought to bear on specific applications. To do so usually requires a physically based model or equation that can relate the laboratory conditions to the mission loading and exposure conditions. An analogy can be made to time-temperature parameters that relate higher-temperature, shorter-time laboratory stress rupture results to longer-time, lower-temperature mission loading exposure. Available time-temperature parameters are generally consistent with the concepts of activation energy for thermally governed time-dependent creep processes. If models are not available for a smooth transition between laboratory and service conditions, extreme or bounding approaches may be necessary.

As an example, suppose the concurrent degradation in service is fretting. Alloy coupons could be prepared with surfaces that have been independently fretted to varying degrees. Subjecting these coupons to subsequent fatigue tests will demonstrate the effects of fretting as though it were a preexisting influence. Testing in this step-wise sequence imposes all of the fretting damage at the beginning of the test, and it could be expected to cause the maximum damage and, hence, a lower-bound fatigue life. This testing philosophy assumes no concurrent synergy between accumulation of fretting damage and accumulation of fatigue damage. Similar evaluations are possible for effects of nuclear radiation on bulk properties (causing, for example, increased strength and decreased ductility) or oxidation on surface-related effects (decreasing surface resistance to cracking). One should not discount the option of testing with a few multiple steps, for example:

- Apply static oxidation to a specimen in a furnace for a time interval.
- Follow this with rapid fatigue cycling for a predetermined block of cycles.
- Remove the specimen from the fatigue machine.
- Reinsert the specimen into the furnace for an additional time interval.
- Reinstall the specimen in the fatigue machine for an additional block of cycles.
- Repeat this process until the specimen fails due to oxidation-accelerated fatigue.

While this procedure is manpower intensive, total testing time in a fatigue machine could be greatly reduced while developing data that are far more relevant to the missions.

Active Loading-Related Effects. A number of active loading variables also fall into the category of concurrent variables. Prime examples of active loading variables are applied mean stresses, multiaxial stress-strain states, cumulative fatigue damage (not constant) loadings, and temperature-related effects such as creep fatigue and TMF. Creep fatigue and TMF are of such significance and require so many changes to conventional fatigue testing procedures that they merit separate discussion.

Mean Stresses. Perhaps the most commonly considered variable for fatigue testing is the mean stress. Mean stress effects on fatigue were recognized by Gerber (Ref 51) as early as the 1870s and have been a source of concern since. One of the most recent thorough reviews

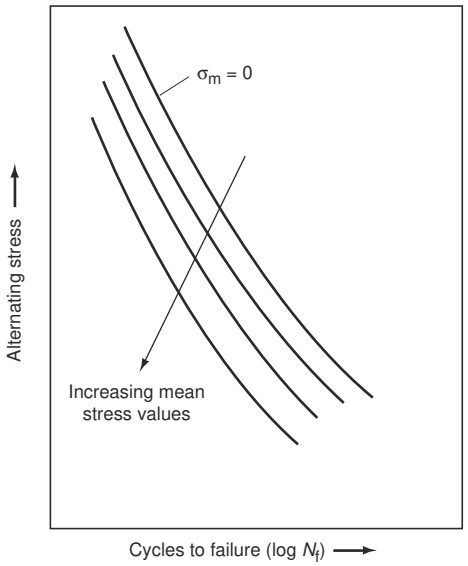

Fig. 23 Schematic axial fatigue curve illustrating the effect of tensile mean stress. After Ref 52

of the subject is given by Conway and Sjodahl (Ref 52).

A typical mean stress evaluation test would be conducted under load control of axial or plane bending in the nominally elastic high-cycle fatigue regime. Under plane bending, one surface has a tensile mean stress whereas the opposite surface has a compressive mean stress of equal magnitude. It is not possible to run independent tensile or compressive mean stress bending fatigue tests. Because tensile mean stresses are typically more damaging than compressive mean stresses, the bending specimen would always initiate fatigue cracks from the tensile mean stress surface. The plane-bending fatigue test is inappropriate for studying mean stress effects in the lower cycle-to-failure regime. Once small amounts of inelasticity occur at the outer surfaces, stress relaxation and redistribution occur and the local mean stresses are no longer directly proportional to the imposed mean loads. In fact, the load amplitude and mean will not change as a result of the local changes in stress, and the test engineer will be unaware of any changes to the stresses. Note that it is not possible to conduct mean stress studies under rotating-bending fatigue.

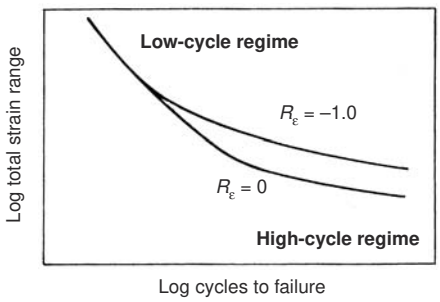

Fig. 25 Schematic illustration of mean-strain cycling effects on low-cycle fatigue resistance. Mean stresses relax to zero at large strain ranges but remain at low strain ranges, thus reducing life.

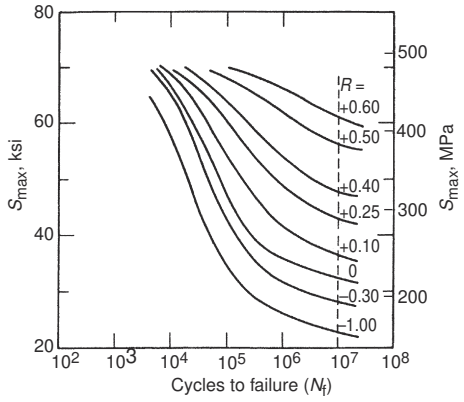

Fig. 24 Effect of tensile mean stresses on axial fatigue resistance of 2024-T3 aluminum alloy at room temperature. After Ref 52

To avoid the problems of bending, axial loading is the recommended mode of testing for mean stress effects. Figure 23 schematically illustrates the decrease in alternating-stress fatigue resistance as the tensile mean stress increases. Frequently, the fatigue curve is displayed in terms of the maximum applied stress in the cycle. Figure 24 shows typical results of the effect of the stress ratio, R (algebraic minimum/algebraic maximum), on the axial fatigue resistance of 2024-T3 aluminum alloy at room temperature over the life range of 10^4 to 10^7 cycles to failure (Ref 52). Care should be taken when mean stresses are applied under load control at very high maximum tensile or compressive stresses. Too high a stress can cause yielding and, hence, cyclic ratcheting in the direction of the mean stress. If in tension, this can lead to eventual excessive tensile strain, subsequent tensile necking (as in a tensile test), and failure long before fatigue cracks have an opportunity to form and grow. Unless an extensometer is employed, small but damaging amounts of ratcheting may escape detection.

Mean loading effects in the low-cycle fatigue regime are best dealt with under strain control. The strain control mode rules out ratcheting, although initial mean stresses imposed by mean straining do have an opportunity to cyclically relax. When imposed strain ranges are large enough that the inelastic strain range is on the order of a tenth of the total or elastic strain range, it is very probable that any initial mean stress will cyclically relax to zero, that is, become completely reversed, even though the straining is not completely reversed (Ref 53). In the high-strain, low-cycle fatigue regime, there is little, if any, effect of mean strain on fatigue life for ductile alloys. However, as the strain range is decreased and the life increases, a nominally elastic condition is reached. Then, a tensile mean strain will be accompanied by a directly proportional tensile mean stress, and the fatigue life will decrease compared to a completely reversed strain cycle. The end result is shown schematically in Fig. 25. Typical data of this nature have been reported for a high-temperature gas turbine engine alloy in (Ref 54).

Multiaxiality. Investigation of multiaxial stress and strain states on fatigue resistance is a perennial issue because the cyclic stress-strain states at critical locations in machinery components are rarely uniaxial. However, the vast majority of fatigue tests are performed using uniaxial loading. The issues involved are so extensive that the subject has merited a separate article ("Multiaxial Fatigue Testing") in this Volume and will not be discussed further in this article.

Cumulative Fatigue Damage. Commonly employed cumulative fatigue damage tests involve random, or nonsteady, loading wherein both the amplitude and mean value of the loading vary continuously (Fig. 26a). Such tests are attempts to simulate in the laboratory the detailed loadings encountered in service. The sequence of loading is commonly referred to as spectrum loading. Also common are simplified, or compressed, loading patterns that have been shown analytically to account for the equivalent amount of fatigue damage that existed in the more complex spectrum loading. These compressed loading patterns capture the basic

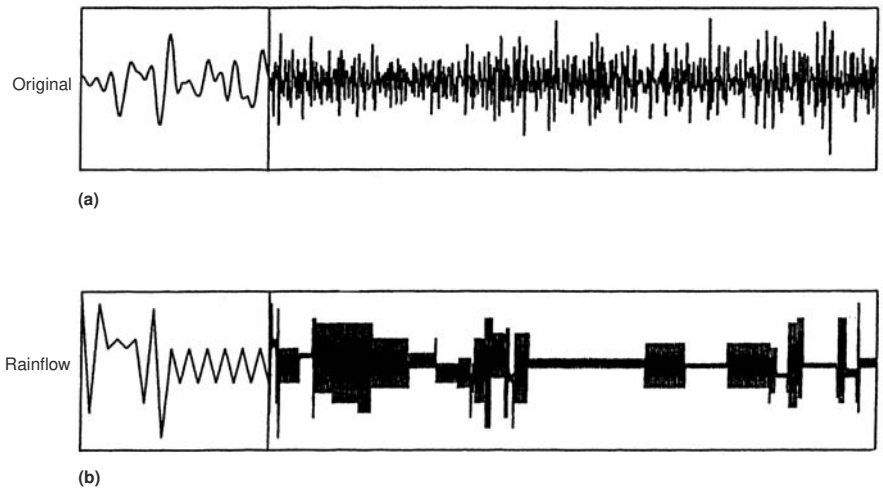

Fig. 26 Nonsteady fatigue loading. (a) Random-appearing original loading pattern. (b) Loading pattern reconstructed by rainflow method of cycle counting. After Ref 55

profile of loading. An illustrative schematic example is shown in Fig. 26(b). In this instance, the simplified loading pattern is arrived at by an equivalent rainflow cycle counting technique (Ref 55). Obviously, reducing the number of loading levels permits simplification of testing. Because a loading pattern may repeat itself, the fatigue loading can be applied in the form of repetitive blocks. Terrestrial-based vehicles, aerospace airframes, and civil engineering structures such as bridges typically experience random loadings during their fatigue crack initiation lifetimes. Greater details on how to approach complex cumulative fatigue damage assessment and testing can be found in Ref 56.

In the extreme are cumulative fatigue damage tests that involve only two loading levels, one in the low-cycle fatigue (LCF) regime, the other in the high-cycle fatigue (HCF) regime. Using this highly simplified testing pattern, it has typically been observed that LCF cycling (to a fraction of the expected life) followed by HCF cycling to failure reduces overall life, and the reverse loading order increases overall life. This is referred to commonly as the classic loading order effect (Ref 57, 58) and is illustrated in Fig. 27. This effect is not captured by linear damage assessment. Consequently, nonlinear cumulative fatigue damage models have proliferated (Ref 58) since Miner's linear damage rule was published in 1945 (Ref 59). The accuracy and viability of any cumulative fatigue damage rule hinges on the assumption that the physical mechanism of damage does not change as loading levels are changed. Clearly, understanding the damage mechanisms is an important and necessary step in the development of accurate models.

Cumulative fatigue damage testing can also involve more than just loading level variations. Changes in the type of loading—for example, thermomechanical and isothermal (Ref 60), axial and torsion (Ref 61), and fatigue and creep-fatigue (Ref 62)—during testing may also be of importance.

Temperature-related effects such as creep-fatigue and TMF are of such significance, and require so many changes to conventional fatigue testing procedures, that they merit separate discussion in the following sections.

Creep-Fatigue Interaction

Creep-fatigue interaction testing and modeling have been intense activities since the late 1950s. Interest was spawned by the introduction, and seemingly premature failures, of components in structural equipment operating at elevated temperatures. Examples include aeronautical gas turbine engines; steam turbines; nuclear reactors and pressure vessel and piping components for electric power generation and chemical processing plants; casting and forging dies; railroad wheels subjected to brake-shoe application; automotive cylinder heads, exhaust valves, manifolds, and exhaust piping systems; and reusable rocket engines. In many cases, the elevated temperature of operation is reasonably constant (isothermal) over a period of time while components are under load and can suffer creep or stress-relaxation processes that hasten crack initiation and early growth. The modes of cracking have frequently exhibited creep-like fractures intermixed with cycle-dependent fatigue-type cracking. Hence the descriptive name, creep-fatigue interaction.

Extensive reviews of creep-fatigue interaction were prepared in the early 1980s (Ref 63–65). Over the intervening decades, more than 100 models or their variations have been proposed to describe creep-fatigue interaction (Ref 66, 67). As many as a dozen of the models have survived and have been applied to practical situations. The three most widely used are the time- and cycle-fraction rule from the ASME Code Case N-47-23 (Ref 68), strain-range partitioning (SRP) (Ref 69) and its total strain version (Ref 70), and continuous damage mechanics (Ref 71).

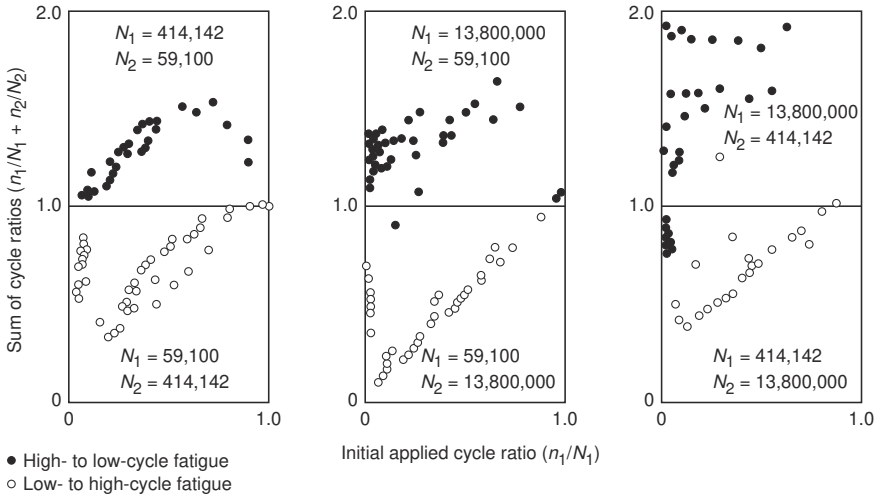

Fig. 27 Examples of classic loading order effect in two load level tests of British aluminum alloy D.T.D. 683. Source: Ref 57

The fatigue machines and associated equipment normally used for creep-fatigue experiments are essentially the same as those used for baseline fatigue tests. Current practice calls for axial loading of a uniform-gage length specimen mounted in a closed-loop servocontrolled fatigue testing machine with provisions for heating the sample to elevated temperatures. Closed-loop strain-controlled testing is most commonly used; when it is not used, strain limit control is imposed to prevent creep ratcheting. The major difference between creep--fatigue and baseline isothermal fatigue testing is in the time per cycle. To introduce creep into the cycle, the frequency is reduced by cycling at a lower strain rate or by introducing a hold period at some selected point within each cycle. Most commonly, a hold period is inserted at the peak strains in a cycle, that is, at maximum or minimum algebraic strains, or at both peaks.

Creep-fatigue interaction testing is conducted at a high enough isothermal temperature that thermally activated, diffusion-controlled creep deformation mechanisms can operate under stress as a function of both time and temperature. As a rough rule of thumb, the transition temperature for creep is on the order of half the absolute melting temperature of an alloy. In earlier years, creep-fatigue testing was conducted to simply ascertain the extent of the damaging effect of creep on cyclic (fatigue) life. Today, tests are still run for that purpose, but more often than not, creep-fatigue testing is designed also to evaluate and calibrate the constants in a viable creep-fatigue life prediction model.

The addition of creep to a cycle of normal fatigue loading will invariably reduce the cyclic life, although the clock time to failure may remain constant or actually increase. Conversely, the superposition of fatigue cycling and conventional monotonic creep will also alter the rate of creeping and the time to rupture. Because of the importance placed on knowing the values of stress and time-dependent deformation, it is generally regarded that creep-fatigue testing be done with axially loaded specimens equipped with extensometry. While some interspersed creep-fatigue testing, that is, repeated blocks of brief periods of creep followed by brief periods of fatiguing, has been reported (Ref 62), the most common tests involve repeating cycles of straining with hold periods imposed in tension or compression alone or in combination. The hold periods may be under constant strain or constant stress. If under constant stress, strain limits are generally imposed to preclude ratcheting. Alternatively, creep could be introduced by controlled slow straining rates in tension, compression, or both.

Figure 28 illustrates the various isothermal hysteresis loops that are commonly encountered in fatigue and creep-fatigue testing. Figures 28(a), (e), (f), and (g) were used to generated the data shown in Fig. 29 for AISI type 304 stainless steel (Ref 67). Here the inelastic strain range is plotted against cycles to failure on log-log coordinates. As can be seen, signifi-